Environmental Science & Technology

pubs.acs.org/est

Article

DNAPL Detection and Delineation with the Radon-Deficit Technique: Analysis of Applicability and Limitations with a Real Case-Study

Fernando Barrio-Parra,* Humberto Serrano-García, Miguel Luri, Miguel Izquierdo-Díaz, and Eduardo De Miguel

Cite This: *Environ. Sci. Technol.* 2025, 59, 26796−26805

Read Online

ACCESS | Metrics & More | Article Recommendations | Supporting Information

ABSTRACT: This study investigates the application of the radon-deficit technique as a real-time screening tool for detecting and delineating Dense Non-Aqueous Phase Liquids (DNAPLs) at a creosote-contaminated site. Traditional site characterization methods often fail to capture the spatial complexity of subsurface contamination. The radon-deficit method makes use of radon gas's preferential partitioning into DNAPL phases to identify contamination zones. A field study involving 558 measurements of ^{222}Rn in soil gas conducted during two years at a former railroad tie treatment facility validated the technique's effectiveness, revealing previously undetected DNAPL accumulations beyond an impermeable barrier that was supposed to be containing the DNAPL accumulation. Subsequent campaigns demonstrated its predictive value for guiding monitoring well placement. Laboratory and modeling studies further clarified radon transport dynamics, suggesting that specific boundary conditions, such as deep geological radon sources, significantly influence the spatial range of applicability of the radon-deficit technique. These findings highlight the technique's effectiveness in refining sampling strategies and enhancing the understanding of DNAPL migration patterns in complex subsurface environments.

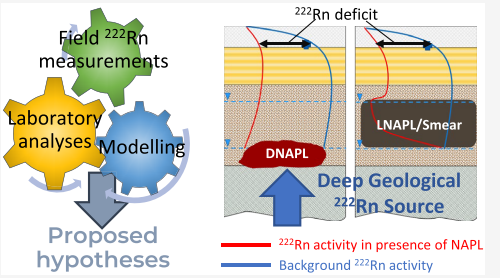

KEYWORDS: *site characterization, creosote, screening, contamination mapping, DNAPL, partition*

1. INTRODUCTION

Traditional methods of characterizing contaminated sites, which rely on high quality, but spatially limited data acquired from a small number of boreholes, soil cores, and groundwater samples, often exhibit deficiencies in accurately representing the intricate dynamics of subsurface contamination phenomena. This is particularly evident when dealing with Dense Non-Aqueous Phase Liquids (DNAPLs).[1−5]

The ^{222}Rn deficit technique (RDT) is a characterization technique that operates in near real-time that can help to increase the density of spatial information and optimize the subsequent and inevitable drilling, sampling and analytical efforts.[6] Radon is a radioactive gas produced by the decay of radium which, in widely varying concentrations, is present in all geologic materials.[7] When radon is produced in the vadose zone, it enters the pore space between mineral grains where it partitions between the air and water phases. When a separate, nonaqueous organic contaminant phase is present, radon preferentially partitions into it with a resulting reduction of what would otherwise be the background radon concentration in soil gas in that area. In the absence of confounding factors such as lateral changes of lithology,[8] this reduction (i.e., deficit) in radon concentration in soil gas can be used to detect and delineate subsurface accumulations of organic contaminants.[9−13] Field measurements of ^{222}Rn in soil gas can be obtained using portable instruments that require minimal drilling and a short data collection time. This characteristic makes the radon-deficit technique a promising screening tool for effectively delineating subsurface organic pollution processes, which helps optimize characterization and monitoring efforts conducted through intrusive methods.

The equation governing radon transport in the vadose zone includes terms for production and partitioning, decay, diffusion, and advection.[9,14,15] The advection term is typically neglected because atmospheric pressure gradients are only relevant within the first few decimeters of the soil.[16−26] Therefore, atmospheric pressure gradients should not influence radon behavior at the standard sampling depths of approximately 1 m. Diffusion-only models present a significant theoretical constraint: the effective diffusion length of radon in porous media is estimated in the range of 0.5 m for sandy soils

Received: October 2, 2025
Revised: November 14, 2025
Accepted: November 17, 2025
Published: December 2, 2025

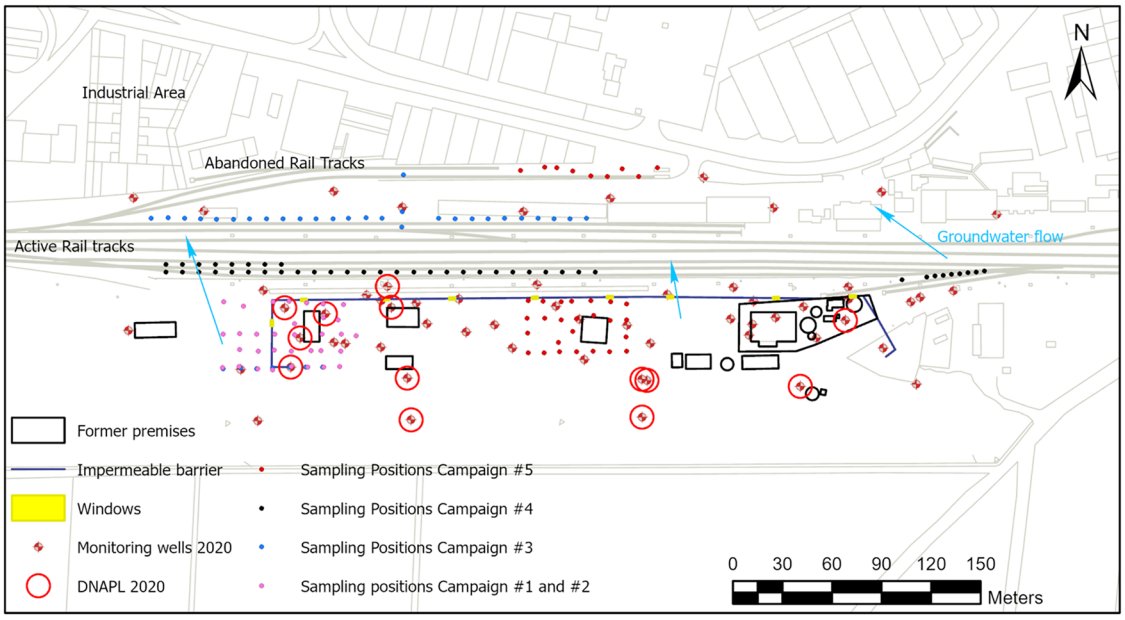

Figure 1. Study area with spatial distribution of (i) monitoring wells installed to collect groundwater samples and locate the DNAPL contamination, (ii) detected DNAPL in June 2020, (ii) former premises of the railroad tie treatment plant, (iv) location of impermeable barrier, (v) groundwater flow directions, and (vi) soil gas ^{222}Rn sampling positions during the different field campaigns.

and 2 m for gravel.[6,27] This implies that a decrease in ^{222}Rn activity produced by the presence of NAPL should only be detectable directly above or in close proximity to the contaminant source.[28,29]

The scientific literature provides numerous examples of the successful application of the radon-deficit technique to assess sites impacted by Light Non-Aqueous Phase Liquids (LNAPLs) at shallow depths, in which the gas sampling point is close to the location of the NAPL.[8,10,12,30−41]

On the other hand, until recently only limited and inconclusive evidence had been reported regarding the application of the ^{222}Rn deficit technique for characterizing DNAPL-impacted sites through soil gas sampling in the vadose zone.[42] Several recent studies, however, have suggested that it can be successfully implemented under specific site conditions.[29,43,44] More commonly, the RDT has been applied using measurements of radon in groundwater, instead of soil gas, using existing networks of monitoring wells.[45−48] Groundwater-based radon monitoring avoids limitations associated with radon diffusion length and temperature-induced variability in the vadose zone,[6] but its dependence on preinstalled wells restricts its applicability in previously uncharacterized areas.

Despite the constraints imposed by radon transport in unsaturated media and the inconclusive outcomes reported in earlier studies, the results presented here—derived from blind field campaigns at a creosote-contaminated site—suggest that the radon-deficit technique may offer a viable approach, under specific site conditions, for the preliminary delineation of DNAPL contamination.

The primary objective of this study is to assess the feasibility and boundary conditions for applying the ^{222}Rn deficit technique to real-time detection and spatial delineation of DNAPL contamination using soil gas measurements. Through a blind case study at a creosote-impacted site, we aim to demonstrate the operational potential of the method and to elucidate the mechanisms that govern its performance in the vadose zone.

2. METHODS AND MATERIALS

2.1. Study Area and Contaminants of Concern. The site under study is a former railroad tie treatment plant which operated between 1938 and 1995 (Figure 1). Historically, creosote (a.k.a. Coal tar oil, Brick oil, Naphthalene oil), a byproduct obtained from the high-temperature processing of coal to make coke or natural gas, was employed as a wood preservative. With a density between 1.00 and 1.17 g/cm^3 creosotes are black or dark brown water-immiscible liquids or semisolids with a naphthalene-like odor. Its composition is variable between creosotes and consists of complex mixtures of hundreds of individual compounds, including aliphatic hydrocarbons, light aromatic compounds (i.e., benzene, toluene, ethylbenzene, and xylene), phenolic compounds and most notably polycyclic aromatic hydrocarbons (PAHs), which can constitute up to 90% by weight of creosote. Some of the PAHs identified in creosote are anthracene, benzo(a)anthracene, benzo(a)pyrene and pyrene, but naphthalene is by far the most abundant. Chronic exposure to creosote can lead to cancer in humans and animals and is also lethal in acute exposures to aquatic organisms.[49−51] Although many hydrocarbons present in the creosote mixture are less dense than water and cease their downward migration upon reaching the water table, creosote products with densities slightly above unity may be able to penetrate as an immiscible phase and continue migrating below the water table.[52] At the study site, a creosote DNAPL accumulation exists that reaches an apparent thickness between 1 and 150 cm in the most contaminated groundwater monitoring wells. The presence of DNAPL in the saturated zone has been shown to vary over time. Detections in one sampling period often do not recur in the next for the same monitoring well, and vice versa.

The lithological sequence at the site consists, from top to bottom, of a 0.5−1 m sand and gravel anthropic backfill

https://doi.org/10.1021/acs.est.5c13917
Environ. Sci. Technol. 2025, 59, 26796−26805

Table 1. Summarized Description of ^{222}Rn Sampling Campaigns[a]

field campaign	date	number of Probes installed	^{222}Rn measurements				number of field replicates	mean soil conditions		mean atmospheric conditions	
			N	min.	mean	max.		humidity	temperature	temperature	pressure
#1	22−25 February 2021	32	135	<500	10,626	48,100	5	NA	NA	15.6	991.9
#2	4−7 May 2021	32	192	<500	13,007	87,900	6	NA	NA	24.9	991.5
#3	13−16 September 2021	37	119	1300	25,660	84,900	4	22	26	25.6	974.8
#4	19−22 October 2021	43	59	<500	13,894	45,700	1	15	22	26.1	992.7
#5	23−26 May 2022	34	53	700	28,519	52,800	6	15	29	28.3	992.7

[a]Descriptive statistics of ^{222}Rn measurements (Bq/m^3) at 0.8 meters below ground level (mbgl), soil and atmospheric conditions - humidity (%), temperature (°C) and pressure (mbar) -. NA: Not Available.

followed by a 1.5−3 m layer of silty clay, 1−2 m of silty sand, and 1−3.5 m of gravels with a sandy matrix, underlain by greenish gray marl at a depth of 7 to 8 m below ground surface (mbgs) that act as an impermeable layer and controls the mobility of the DNAPL. The thicknesses of these layers vary significantly across the site. The groundwater table at the time of the study lied at approximately 6 mbgs and the groundwater flow through the gravel layer follows a north−northwest direction. Accompanying the groundwater flow, a plume of dissolved contaminants (with concentrations of benzene and naphthalene ranging between 30−300 and 70−7000 ug/L respectively) reach an industrial area bordering the study area to the north. The DNAPL accumulates in the permeable gravel level, confined by the underlying impermeable marl. In some areas, where buildings in which creosote operations were located, the soils are affected by the presence of organic contamination with vertical migration patterns affecting the unsaturated profile (i.e., down to depths of about 5 m).

Since the detection of creosote contamination in 2007, several efforts have been made at the site to characterize and contain the migration of DNAPL through the gravel layer. In 2010, the spatial distribution of the contamination was believed to be well-known, and it was decided to build an impermeable barrier to contain the advance of the DNAPL. The bentonite cement barrier, which was installed in December 2011, is 9 m deep, 0.45 m thick, and penetrates 2 m into the impermeable marl. It incorporates 9 openings to allow clean groundwater circulation. When the barrier was built, the groundwater table lied at 5 mbgs, so the 2 m wide openings were opened from 0.0 to 5.5 m below ground level. Nowadays these "windows" are no longer operational due to a drop of the water table caused by overexploitation of the aquifer and long-lasting regional droughts. By 2020, prior to the radon deficit studies, 60 groundwater monitoring wells had been installed at the site.

2.2. Sampling and Analysis. A total of five ^{222}Rn sampling campaigns were carried out in the study area (Table 1). The objective of campaigns #1 and #2 was to validate the radon-deficit technique using blind surveys, i.e., conducting campaigns without the researchers having any information on the presence or absence of DNAPL, and a posteriori validation of the results using information provided by the site managers. Once the technique was validated, campaigns #3 to #5 were used with a predictive purpose, i.e., to guide the sampling design in areas where direct information from boreholes about NAPL pollution was lacking. The inferred information on possibly contaminated areas obtained with the radon-deficit technique was used to position new monitoring wells with which to confirm the presence or absence of DNAPL. The design of the sampling network in each campaign, as well as the spatial representation of the DNAPL distribution at the site known prior to the start of the work, is shown in Figure 1.

Field measurements were carried out as follows (a more detailed description of the field methodology can be found in García-González et al.[41] and Barrio-Parra et al.[43]): Stainless-steel, hollow rods equipped with lost tips were driven into the ground to a depth of approximately 0.8−0.9 m. At that depth, the lost tip was disengaged opening a gap through which, after purging, 150 mL of soil gas was collected with a syringe and introduced in a vacuum-ready detachable ionization chamber. After a standing time of 15 min (to allow thoron (^{220}Rn) to decay), the chamber was connected to a RM-2 pulse ionization detector (RADON v.o.s.), and the activity of radon in the sample was registered after the ionization current generated by α radiation from the decay of ^{222}Rn was measured over a 120-s interval. The signal is processed by the reader using a calibration constant derived from a factory calibration performed in a radon chamber traceable to international standards. The RM-2 system operates within a measurement range of 3 to 1200 kBq/m^3 and offers a detection resolution of 100 Bq/m^3. To assess the replicability of the measurements, 11 measurements were replicated during campaign #2 with two different detectors at the sampling position. A comparison of means test (Tukey's test) showed no statistically significant differences between the measurements performed with each instrument (p-value = 0.7).

The separation between sampling points was always 10 m. For that dense sampling spacing, once the steel rods were in place, a total of approximately 15 measurements per hour were registered. If the sampling point presented a low pneumatic permeability (e.g., due to the presence of clays at the sampling depth) the point was reinstalled in the vicinity of the original sampling position. Previous studies have shown the relationship between atmospheric temperature at ground level and the registered ^{222}Rn concentration.[29,44,53] To minimize the influence of this confounding factor, series of successive measurements of ^{222}Rn were conducted and the mean value of the measurements at each point was considered for interpretation. The number of field replicates is specified for each field campaign in Table 1.

https://doi.org/10.1021/acs.est.5c13917
Environ. Sci. Technol. 2025, 59, 26796−26805

The conditions and details of each experimental campaign are summarized in Table 1 and spatially represented in Figure 1. The first sampling campaign was aimed at validating the radon deficit technique in an area divided in two by the impermeable barrier: One half of the area, within the barrier, presented a known DNAPL accumulation (under a former site facility); the other half, outside the barrier, was assumed to be free of DNAPL (Figure 1). Given the unexpected results (see discussion below) of this first campaign, the decision was made to replicate the same sampling grid during campaign #2. Once the method had been validated, the following campaigns were designed to obtain preliminary information for deciding the location of new monitoring wells to intercept the potential northwest DNAPL migration. The sampling profiles were located in areas where there had been no historical contamination sources, i.e., if DNAPL were present, it could not have originated in situ. During campaigns #3 to #5, soil temperature and humidity were recorded with a TEROS11 (METER Group) placed at a depth of 30 cm.

Lastly, groundwater samples and samples of DNAPL were collected from two monitoring wells, one with 152 cm and the other with 0.5 cm of DNAPL at the bottom of the water column. To confirm the hypotheses that a light NAPL emulsion could be segregating from the DNAPL body, the water samples were taken at two depths (near the top of the water column in the monitoring well and right above the DNAPL accumulation at the bottom). Samples were taken with a peristaltic pump at a low-flow rate of 0.5 l/min at depths of approximately 6.5 m ("Top" sample) and 7 m ("Bottom" sample). These depths were selected based on site-specific hydrogeological conditions: the water table was located at approximately 6.2 m, and the impermeable base of the gravel aquifer was identified at a depth of around 7.5 m. The concentrations of aliphatic and aromatic hydrocarbon fractions, the USEPA's (US Environmental Protection Agency) 16 priority-pollutant PAHs,[54] and benzene, toluene, ethylbenzene, and xylenes were determined by gas chromatography (GC-FID and GC-MS). In addition, a simple partitioning experiment was carried out in the laboratory. For this purpose, a sample (1/3 by volume) of the DNAPL extracted in the monitoring wells during the remediation processes and a sample of commercial creosote (CAS Number 8021-39-4) were placed in two vials and made up to 50 mL with water (2/3 by volume). The vials remained at room temperature and without shaking for one year (from November 2023 to November 2024). After this standing time, the vials were inspected and photographed to check if a light NAPL had developed.

2.3. Modeling. To evaluate the influence of site-specific factors on the performance of the radon-deficit technique, the 1D_RnDPM model[29] was employed, a one-dimensional numerical tool that simulates ^{222}Rn production, partitioning, and diffusive transport in unsaturated porous media. The model solves the radon mass balance equation considering radioactive decay, temperature-adjusted production, and phase partitioning between air, water, and NAPL. Transport is assumed to occur exclusively by diffusion, neglecting advective fluxes, which are considered negligible at the sampling depths used in this study.[8,33]

The model requires site-specific input parameters, which were derived from laboratory analyses of soil samples collected during field campaigns. These included equilibrium radon activity (C_{eq}), bulk density (ρ), and total porosity (θ_t), determined following the methodology described in Barrio-Parra et al.[29] The radon emanation rate was calculated from accumulation chamber experiments, and porosity was estimated from gravimetric measurements for two solid samples of about 1 kg from the anthropic backfill and silty-clay layers obtained from soil cores at the site. In the model, the vertical profile was discretized into two layers (1 m of anthropic backfill, and a 5 m-thick subsurface layer of silt) each characterized by its own physical properties following the methodology described by Barrio-Parra et al.[29]

Simulations were conducted under the assumption of a dry soil profile (i.e., zero water-filled porosity) to isolate the effect of NAPL on radon partitioning. To study the theoretical effect of the presence of DNAPL in the soil profile two sets of simulations were performed. Simulation #1 assumed a clean soil profile with no DNAPL, while in Simulation #2 a residual DNAPL saturation of 0.002[9] was assumed in the first 1m of soil above the water table, in accordance with the analytical information obtained from boreholes in the study area (see Section 3.2). Partition coefficients were set at 4.4[20] for air–water (K_H) and 13[33] for air–NAPL (K_n). A Dirichlet boundary condition was assumed in the upper part of the profile with a ^{222}Rn activity of 0 Bq/m^3 representing the atmospheric dilution process. For each simulation, two types of lower boundary conditions were tested to assess their influence on simulated radon profiles: (i) a Neumann condition (zero-flux), and (ii) a Dirichlet condition with fixed radon activity at depth. The latter was introduced to evaluate whether elevated radon concentrations at the base of the profile—potentially associated with deep geological sources or uranium enrichment—could reproduce radon activities within the range observed in the field.

The comparison of the ^{222}Rn activities predicted by these simulations with the empirical measurements at the site were employed to evaluate hypotheses about the theoretical radon transport processes that could explain the obtained field results.

3. RESULTS

3.1. Field Campaigns. This section describes the sequence of results obtained during consecutive data collection campaigns in the study area and how they align with direct observations of DNAPL presence and thickness in monitoring wells. The first two sampling campaigns were blind studies, meaning that site managers did not disclose to the authors any prior information about the distribution of the DNAPL at the site.

To validate the applicability of the radon-deficit technique, the site managers proposed sampling on both sides of the impermeable barrier in Campaign #1. According to the preliminary conceptual model, site managers were aware of the presence of a DNAPL on the eastern (inner) side of the barrier and believed that the western (outer) side was free of contamination since no DNAPL had been detected in the few monitoring wells installed on this side (Figure 1). During the ^{222}Rn-deficit campaign, two areas of negative anomalies were detected, one to the east of the barrier and the other to the west. Given the disagreement between the ^{222}Rn-deficit results and the assumed distribution of the DNAPL, which was supposed to be present only in the eastern half of the study area, confined inside the impermeable barrier, and absent from

https://doi.org/10.1021/acs.est.5c13917
Environ. Sci. Technol. 2025, 59, 26796−26805

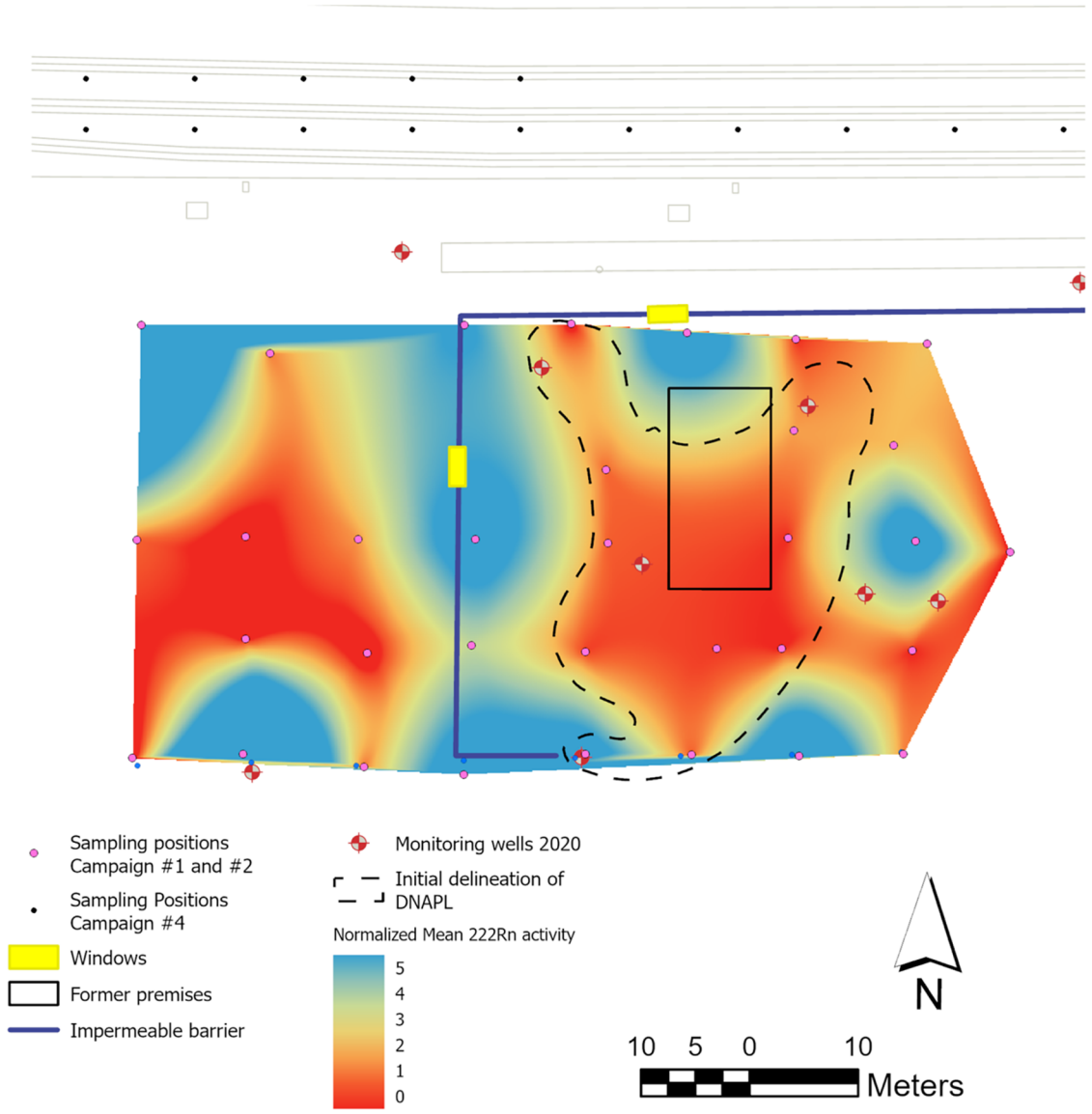

Figure 2. Normalized mean ^{222}Rn activity surface map obtained during Campaign #2 with a Nearest Neighbor Interpolation. The data obtained in each series of measurements was divided by its average so that values above 1 represent points with ^{222}Rn concentrations above the average and vice versa (unitless). Dashed lines represent the delineation of the DNAPL with data from monitoring wells before the first ^{222}Rn deficit technique campaign was undertaken at the site.

the western half, it was decided to replicate the ^{222}Rn measurements in the same area in Campaign #2.

As shown in Table 1, the mean ^{222}Rn activity values were similar in both campaigns, although higher maximum activity values were detected during Campaign #2. This increase in maximum values were probably related to the higher temperatures registered during the second campaign.[13,16,44,55] Figure 2 synthetically presents the results of Campaign #2. Consistent with the results of Campaign #1, two zones with a ^{222}Rn deficit were identified, one to the east of the impermeable barrier (where the presence of DNAPL was already well established) and another one to the west of it. New monitoring wells specifically drilled and installed to verify these results (Figure 3) proved that the second anomaly outside the impermeable barrier was indeed associated with a large DNAPL accumulation that had gone undetected until that moment, and served as confirmation of the applicability of the radon-deficit technique at the site.

The ^{222}Rn concentrations recorded during campaigns #3 and #5 are shown in Figure 4, where low radon levels are clearly surrounded by values similar to or above the mean. These areas of low concentrations were identified as potentially affected by the presence of DNAPL (Figure 3). Sampling of the new monitoring wells installed after the campaign confirmed either the presence of DNAPL, as predicted by the ^{222}Rn deficit technique, or, where DNAPL was absent, high concentrations of dissolved TPHs (Total Petroleum Hydrocarbons) and evidence of smearing in the corresponding soil cores. The presence of an impermeable clay lens at the sampling depth (0.8 m) made the extraction of soil gas impossible in 28 of 35 sampling points during campaign #4, which was discarded.

3.2. Groundwater Chemical Analyses. The detailed results of the chemical analyses of the four groundwater samples collected from two monitoring wells at the site are presented as Supporting Information. As expected, the

https://doi.org/10.1021/acs.est.5c13917
Environ. Sci. Technol. 2025, 59, 26796−26805

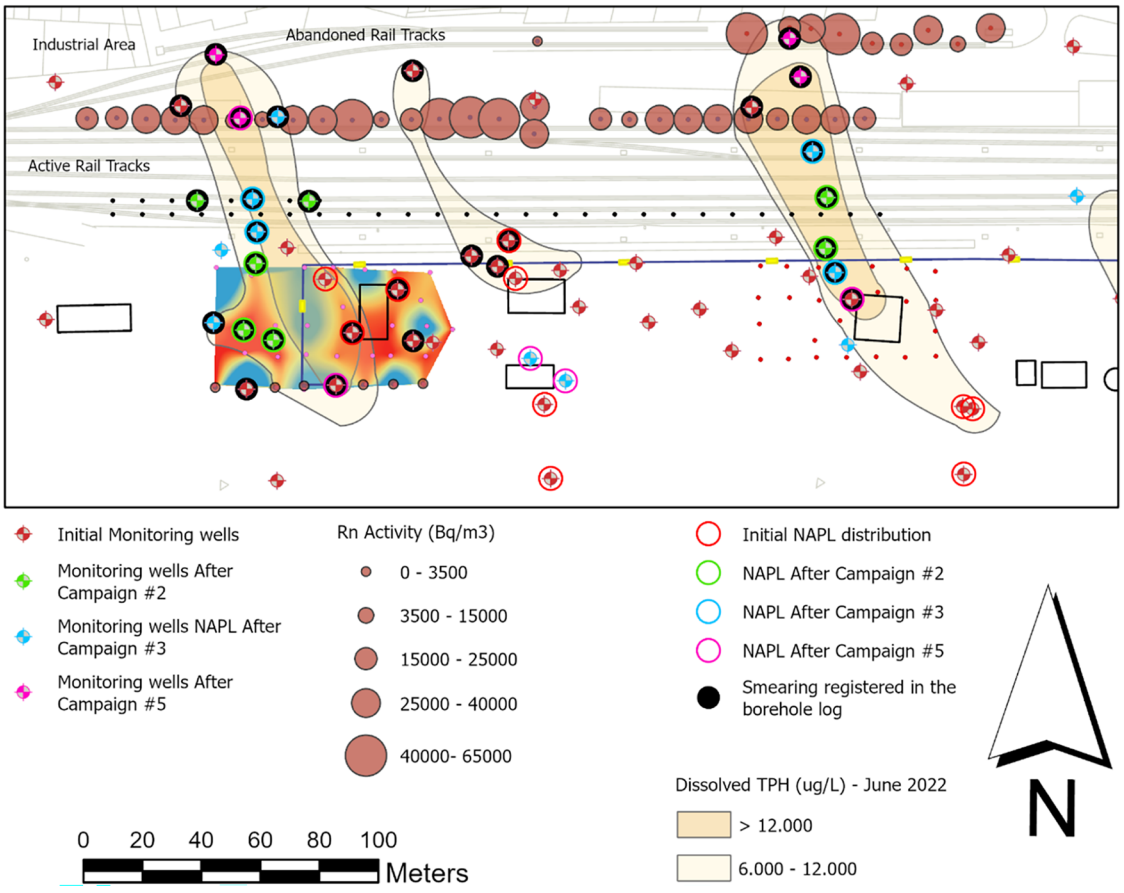

Figure 3. Time evolution of the monitoring well distribution, detected organic contamination and summarized results of the ^{222}Rn deficit field campaigns. Results of Campaigns #3 and #5 are represented as proportional circles (bigger diameters stand for higher ^{222}Rn activities and vice versa). The contours of the dissolved Total Petroleum Hydrocarbons (TPH) measured during June 2022 is also plotted.

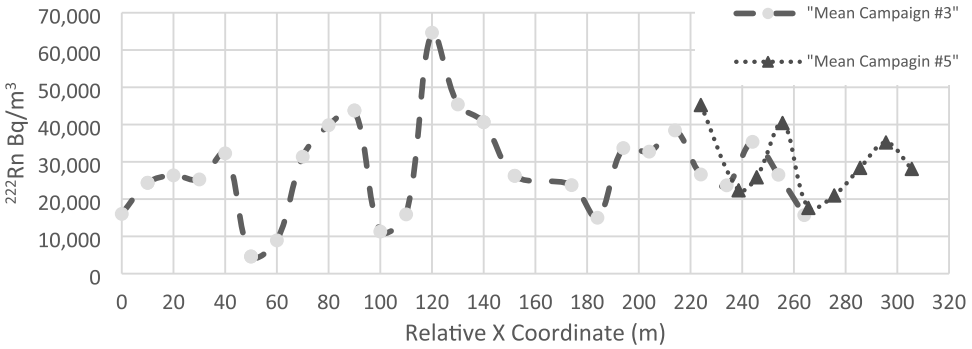

Figure 4. West-East mean ^{222}Rn activity profiles obtained in Campaigns #3 and #5. The origin of X-coordinates has been established at the westernmost point of the profile of Campaign #3. Note that the position of the points of the profile of Campaign #5 are shifted in the Y-coordinate and that here they appear next to those of Campaign #3 due to the two-dimensional representation. The exact position of the sampling points for each campaign can be found in Figure 1.

concentrations of aromatic compounds greatly exceeded those of their aliphatic counterparts. Naphthalene and acenaphthene presented the highest individual concentrations with maximum values of 8100 and 1200 μg/L, respectively. The concentrations of the different aliphatic fractions were similar in both monitoring wells whereas those of aromatic fractions were consistently and significantly higher in the well with the thicker DNAPL layer.

The concentrations of the lighter hydrocarbon fractions, both aromatic and aliphatic, are always clearly below their respective theoretical water solubilities.[56−58] However, the reported dissolved concentrations of aromatic fractions > C16 and aliphatic fractions > C12 are all above their respective water solubilities and although those values cannot be interpreted in quantitative terms, they are strongly indicative of the presence of NAPL in the water column. Of special interest is the fact that aliphatic fractions > C12-C16, > C16-C21 and > C21-C35, all of which have densities below that of water, are reported to reach concentrations in the "Top" samples (i.e., collected immediately beneath the top of the water column) between 2 and 5 orders of magnitude higher than their theoretical water solubilities. This observation lends

https://doi.org/10.1021/acs.est.5c13917
Environ. Sci. Technol. 2025, 59, 26796−26805

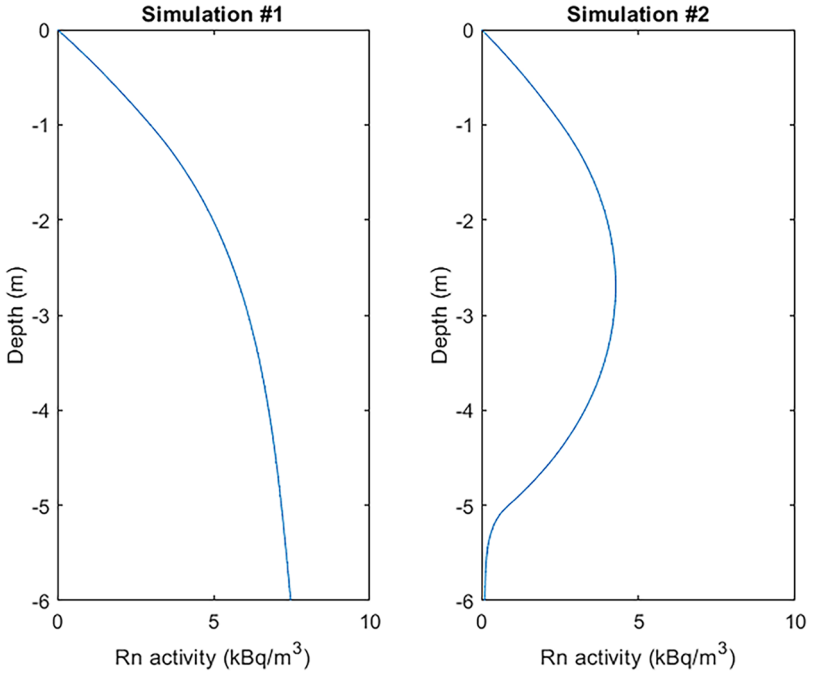

Figure 5. ^{222}Rn activity profiles obtained for simulations #1 and #2 over a 30-day time span with a Newman boundary condition at the bottom.

support to the hypothesis that a light free hydrocarbon phase, segregated from the main DNAPL body, can have developed at the site.

3.3. Modeling Results. In order to obtain the information necessary to perform simulations of the diffusive transport process, generation/decay and partition of ^{222}Rn in the subsoil of the site, laboratory measurements of the equilibrium activity of ^{222}Rn, porosity and bulk density were performed for two soil samples (corresponding to the levels of anthropic fill and clays) following the protocols described in Barrio Parra et al.[29] Equilibrium radon activities of 139.35 and 153.5 Bq/m^3 were obtained for the anthropic and clay levels, respectively. The bulk densities and porosities obtained were 1105.5−1334.2 kg/m^3 and 51−46% respectively for the anthropic fill and clay layers.

To study the vertical evolution of radon activity at the site, two simulations were performed with the 1D_RnDPM model.[29] Simulation #1 assumed a clean soil profile with no DNAPL, while in Simulation #2 a residual DNAPL saturation of 0.002 was considered in the first 1m of soil above the water table. Figure 5 shows the ^{222}Rn activity profiles in the subsurface for both simulations with a Newman (zero-flux) lower boundary condition. The ^{222}Rn activity decreases significantly in the vicinity of the DNAPL and recovers values similar to those obtained for an undisturbed profile at a depth of approximately 5 m. The results of both simulations yield ^{222}Rn activities close to 2000 Bq/m^3 at the sampling depth (0.8 m). This result indicates, on the one hand, that contaminated sections of the soil profile cannot theoretically be distinguished from unaffected ones by sampling at a depth of 0.8 m, and, on the other hand, that the predicted ^{222}Rn activities are substantially lower than those measured in the field (Table 1).

In order to identify the conditions under which the numerical model would yield results similar to those registered in the field (under the hypotheses of ^{222}Rn generation-decay, partition, and diffusion-only transport of the 1D_RnDPM model), the same two simulations were repeated employing a Dirichlet boundary condition for the lower part of the soil profile. By setting a Dirichlet condition of 10^6 Bq/m^3 at a depth of 6 m, activities of 30,000 and 2,500 Bq/m^3 were obtained for simulations #1 and #2 respectively at the sampling depths (0.8 m). These values are in the range of the activities measured in the field (Table 1, Figure 3) and allow to discriminate between contaminated and clean soil sections.

4. DISCUSSION

At the site, the results of the successive ^{222}Rn-deficit campaigns guided the installation of new monitoring wells, which confirmed the presence of previously unknown DNAPL affected areas and zones of residual NAPL saturation (smearing), and marked the extent of the plume of dissolved TPHs. The technique helped to identify sources gone undetected during the initial conventional site characterization, to detect unsuspected contaminant migration toward the north, and to unveil an incorrect design of the retention barrier, thus facilitating and optimizing subsequent investigation efforts.

Most interestingly, ^{222}Rn anomalies associated with the presence of DNAPL at depth were detected in areas where there had been no activities related to creosote production, use or disposal. This finding suggests that the ^{222}Rn deficit technique can identify DNAPL bodies which are not located directly beneath their source zones[43] but have migrated away from them.

A potential explanation for this unexpected result is the development of a light NAPL, segregated from the main DNAPL body at the site. The frequent mention in field records of the presence of an oily sheen on groundwater sampling tools used at the site, the results of the analyses of groundwater samples from wells with DNAPL, and the development of a thin, overlying separate phase in test tubes containing a mixture of commercial creosote and water (Figure A1 in Supporting Information), seem to corroborate the above assumption. The presence of a light NAPL segregated from an

https://doi.org/10.1021/acs.est.5c13917
Environ. Sci. Technol. 2025, 59, 26796−26805

underlying DNAPL accumulation, as suggested by Scherr et al.[50] and corroborated by the laboratory and field observations described above, could smear the vadose zone as the groundwater table fluctuates[59] and the residual NAPL trapped in the smearing zone could create a radon-deficit indirectly associated with the DNAPL present in the saturated zone.

The modeling results at the site are in agreement with previous studies which evaluate the influence of boundary conditions in the ^{222}Rn activity profile in the vadose zone.[9,32,60] These studies emphasize the use of high boundary conditions in the lower part of the profile to fit experimental ^{222}Rn activity determinations in the vadose zone to theoretical generation and transport models.[14,61] This ^{222}Rn activity in the lower part of the profile may have a deep geological origin.[41] Deep ^{222}Rn may be transported to the surface by carrier gases, driven by atmospheric air circulation in the shallow permeable vadose zone, which is influenced by the temperature difference between the subsoil and the ambient atmosphere.[17,18,24−26,44,53] Another possible explanation for the elevated boundary condition at the base of the profile is related to uranium precipitation processes. The application of the ^{222}Rn deficit technique in the exploration of petroleum reservoirs associates uranium precipitation and enrichment around the deposit with the reducing conditions generated by the presence of hydrocarbons. Uranium precipitation could act as a source of ^{222}Rn at depth justifying the use of high lower boundary conditions.[62,63] There are strong indications that this is the case at the study site, where the groundwater is suspected to be significantly enriched in UO_2^{2+} due to the presence of an upstream waste storage deposit suspected of generating leachates with elevated concentrations of dissolved uranium.

Although the Radon Deficit Technique (RDT) is useful for detecting subsurface contamination, it faces significant limitations due to the complex and site-specific variability of ^{222}Rn activity in soil gas. Environmental parameters such as soil moisture, temperature gradients, and atmospheric pressure fluctuations can substantially influence radon measurements, complicating the interpretation of reduced ^{222}Rn concentrations as indicators of NAPL contamination.[16,43,64] These confounding factors are particularly problematic when measurements are taken across different campaigns or seasons, making it difficult to distinguish between natural background oscillations and contamination-induced deficits. Furthermore, the variability in the uranium content of the bedrock and the ^{226}Ra activity may also contribute to fluctuations in soil gas radon background levels, potentially affecting the reliability of RDT.[65,66] These findings underscore the need for further research into the geochemical and environmental controls on radon dynamics to enhance the robustness and interpretative power of RDT in heterogeneous field conditions.

5. IMPLICATIONS

During this study, a combination of field measurements of radon in soil gas, laboratory analysis of soil and groundwater samples, and modeling efforts has allowed to understand the expanded set of circumstances under which the radon deficit technique can effectively detect and delineate DNAPL accumulations. Conventionally, this technique has been considered applicable only when:

(a) the DNAPL body is sufficiently shallow so that the effective diffusion length of ^{222}Rn is not a limiting factor, or

(b) the whole soil profile is smeared by a DNAPL percolating from a shallow source. The residual saturation left behind in the upper soil profile by the percolating DNAPL creates a radon-deficit in soil gas indicative of a DNAPL accumulation at depth.

In both cases, the radon-deficit technique is only useful to detect and delineate the original source zone(s).

Two more circumstances have been identified that expand the range of applicability of the technique to include the detection of DNAPL bodies which have migrated (or are migrating) from the source zone:

(c) A light nonaqueous phase segregates from the advancing DNAPL body and smears the vadose zone as the groundwater table fluctuates. As in case (b) above, the residual NAPL trapped in the smearing zone creates a radon-deficit in soil gas indirectly associated with the DNAPL present in the saturated zone.

(d) High emanation rates at depth result in concentrations of ^{222}Rn in shallow soil gas high enough to make the difference in radon levels in unpolluted areas and areas where the DNAPL is measurable.

Under these circumstances, the radon-deficit technique can trace the presence of DNAPL not only directly beneath its source zone but also along its migration pathways, and it can, therefore, substantially reduce the cost of environmental investigations and the possibility of DNAPL accumulations going undetected by conventional site characterization techniques. To standardize the use of the radon-deficit technique as a screening tool at DNAPL-impacted sites, however, further research is needed to understand and quantify the variations of natural radon concentrations in soil gas with soil temperature and water content given that these oscillations act as strong confounding factors in the interpretation of radon deficits.

■ ASSOCIATED CONTENT

Supporting Information

The Supporting Information is available free of charge at https://pubs.acs.org/doi/10.1021/acs.est.5c13917.

Analytical results of groundwater samples including photographs of DNAPL partition experiments (PDF)

^{222}Rn activities recorded during field campaigns (XLSX)

■ AUTHOR INFORMATION

Corresponding Author

Fernando Barrio-Parra − *Prospecting & Environment Laboratory (PROMEDIAM), Universidad Politécnica de Madrid, 28003 Madrid, Spain;* orcid.org/0000-0001-5475-3567; Email: fernando.barrio@upm.es

Authors

Humberto Serrano-García − *Prospecting & Environment Laboratory (PROMEDIAM), Universidad Politécnica de Madrid, 28003 Madrid, Spain*

Miguel Luri − *Ingénieur Géologue ENSG − Consultant, 28003 Madrid, Spain*

https://doi.org/10.1021/acs.est.5c13917
Environ. Sci. Technol. 2025, 59, 26796−26805

Miguel Izquierdo-Díaz − *Prospecting & Environment Laboratory (PROMEDIAM), Universidad Politécnica de Madrid, 28003 Madrid, Spain*
Eduardo De Miguel − *Prospecting & Environment Laboratory (PROMEDIAM), Universidad Politécnica de Madrid, 28003 Madrid, Spain*

Complete contact information is available at: https://pubs.acs.org/10.1021/acs.est.5c13917

Notes

The authors declare no competing financial interest.

■ ACKNOWLEDGMENTS

This study was financed through the CARESOIL-CM [TEC-2024/ECO-69] research programme of the Regional Government of Madrid (Comunidad de Madrid - Spain) and the Multiannual Agreement 2023-2026 with Universidad Politécnica de Madrid in the Line A, Emerging Ph.D researchers ML-TRACER grant [DOCTORES-EMERGENTES-24-71H88I-60-POKTT9] (Comunidad de Madrid - Spain).

■ REFERENCES

(1) Fernández, J.; Arjol, M. A.; Cacho, C. POP-Contaminated Sites from HCH Production in Sabiñánigo, Spain. *Environ. Sci. Pollut. Res.* **2013**, *20* (4), 1937−1950.
(2) Kram, M. L.; Keller, A. A.; Rossabi, J.; Everett, L. G. DNAPL Characterization Methods and Approaches, Part 1: Performance Comparisons. *Groundwater Monit. Rem.* **2001**, *21*, 10.
(3) Newell, C. J.; Connor, J. A.Detection and Delineation of Subsurface Dnapl Distribution *Water Environ. Found. DNAPL Preconference Semin. WEF* 1992, p 18.
(4) USEPA. *The DNAPL Remediation Challenge: Is There a Case for Source Depletion?*; Kavanaugh, M. C.; Rao, P. S. C., Eds.; National Risk Management Research Laboratory: Cincinnati, OH, 2003.
(5) USEPA. Site Characterization Technologies for DNAPL Investigations. 2004, EPA542-R-04-017.
(6) Sukanya, S.; Noble, J.; Joseph, S. Application of Radon (222Rn) as an Environmental Tracer in Hydrogeological and Geological Investigations: An Overview. *Chemosphere* **2022**, *303* (May), No. 135141.
(7) Cothern, R.; Smith, J. E. *Environmental Radon*; Cothern, C. R.; Smith, J. E., Eds.; Environmental Science Research: New York, 1987.
(8) De Miguel, E.; Barrio-Parra, F.; Elío, J.; Izquierdo-Díaz, M.; García-González, J. E.; Mazadiego, L. F.; Medina, R. Applicability of Radon Emanometry in Lithologically Discontinuous Sites Contaminated by Organic Chemicals. *Environ. Sci. Pollut. Res.* **2018**, *25* (20), 20255−20263.
(9) Höhener, P.; Surbeck, H. Radon-222 as a Tracer for Nonaqueous Phase Liquid in the Vadose Zone. *Vadose Zone J.* **2004**, *3* (4), 1276.
(10) Schubert; Freyer, K.; Treutler, H. C.; Weiss, H. Using Radon-222 in Soil Gas as an Indicator of Subsurface Contamination by Non-Aqueous Phase-Liquid (NAPLs). *Geofis. Int.* **2002**, *41*, 433−437.
(11) Weiss, R. F. *Krypton, Xenon and Radon Gas-Solubilities*; Lawrence Clever, H., Ed.; Pergamon Press: Oxford, England, 1980; Vol. *4*.
(12) Schubert; Paschke, M.; Lau, S.; Geyer, W.; Knöller, K. Radon as a Naturally Occurring Tracer for the Assessment of Residual NAPL Contamination of Aquifers. *Environ. Pollut.* **2007**, *145* (3), 920−927.
(13) Schubert. Using Radon as Environmental Tracer for the Assessment of Subsurface Non-Aqueous Phase Liquid (NAPL) Contamination − A Review. *Eur. Phys. J.:Spec. Top.* **2015**, *224* (4), 717−730.
(14) Orabi, M. Multi-Layer Description Model for Radon Concentration in Soil. *Eur. Phys. J. Plus* **2018**, *133*, 133−135.
(15) Cohen, G. J. V.; Bernachot, I.; Su, D.; Höhener, P.; Mayer, K. U.; Atteia, O. Laboratory-Scale Experimental and Modelling Investigations of 222Rn Profiles in Chemically Heterogeneous LNAPL Contaminated Vadose Zones. *Sci. Total Environ.* **2019**, *681*, 456−466.
(16) Schubert; Schultz, M. Diurnal Radon Variations in the Upper Soil Layers and At the Soil-Air Interface Related To Meteorological Parameters. *Health Phys.* **2002**, *83* (1), 91−96.
(17) Etiope, G.; Martinelli, G. Migration of Carrier and Trace Gases in the Geosphere: An Overview. *Phys. Earth Planet. Inter.* **2002**, *129* (3−4), 185−204.
(18) Yang, T. F.; Chou, C. Y.; Chen, C.-H.; Chyi, L. L.; Jiang, J. H. Exhalation of Radon and Its Carrier Gases in SW Taiwan. *Radiat. Meas.* **2003**, *36* (1), 425−429.
(19) Richon, P.; Perrier, F.; Koirala, B. P.; Girault, F.; Bhattarai, M.; Sapkota, S. N. Temporal Signatures of Advective versus Diffusive Radon Transport at a Geothermal Zone in Central Nepal. *J. Environ. Radioact.* **2011**, *102* (2), 88−102.
(20) Scanlon, B. R.; Nicot, J. P.; Massmann, J. W. Soil Gas Movement in Unsaturated Systems. In *Soil Physics Companion*; Warrick, A. W., Ed.; CRC Press: Boca Raton, Fla, 2002; pp 297−341.
(21) Thomas, D. M.; Cotter, J. M.; Holford, D. Experimental-Design for Soil Gas Radon Monitoring. *J. Radioanal. Nucl. Chem.* **1992**, *161* (2), 313−323.
(22) Antonopoulos-Domis, M.; Xanthos, S.; Clouvas, a.; Alifrangis, D. Experimental and Theoretical Study of Radon Distribution in Soil. *Health Phys.* **2009**, *97* (May), 322−331.
(23) Yakovleva, V. S.; Parovik, R. I. Solution of Diffusion-Advection Equation of Radon Transport in Many-Layered Geological Media. *Nukleonika* **2010**, *55* (4), 601−606.
(24) Durrance, E. M.; Gregory, G. R. Helium and Radon Transport Mechanisms in Hydrothermal Circulation Systems of Southwest England. *Geochem. Gaseous Elem. Compd.* **1990**, 337−352.
(25) Etiope, G.; Guerra, M.; Raschi, A. Carbon Dioxide and Radon Geohazards over a Gas-Bearing Fault in the Siena Graben (Central Italy). *Terr. Atmos. Ocean. Sci.* **2005**, *16* (4), 885−896.
(26) Toutain, J. P.; Baubron, J. C. Gas Geochemistry and Seismotectonics: A Review. *Tectonophysics* **1999**, *304* (1−2), 1−27.
(27) Cohen, G. J. V.; Jousse, F.; Luze, N.; Höhener, P.; Atteia, O. LNAPL Source Zone Delineation Using Soil Gases in a Heterogeneous Silty-Sand Aquifer. *J. Contam. Hydrol.* **2016**, *192* (June), 20−34.
(28) Cecconi, A.; Verginelli, I.; Baciocchi, R. Modeling of Soil Gas Radon as an in Situ Partitioning Tracer for Quantifying LNAPL Contamination. *Sci. Total Environ.* **2022**, *806*, No. 150593.
(29) Barrio-Parra, F.; Hidalgo, A.; Izquierdo-Díaz, M.; Arévalo-Lomas, L.; De Miguel, E. 1D_RnDPM: A Freely Available 222Rn Production, Diffusion, and Partition Model to Evaluate Confounding Factors in the Radon-Deficit Technique. *Sci. Total Environ.* **2022**, *807*, No. 150815.
(30) Hunkeler, D.; Hoehn, E.; Höhener, P.; Zeyer, J. 222 Rn as a Partitioning Tracer To Detect Diesel Fuel Contamination in Aquifers: Laboratory Study and Field Observations. *Environ. Sci. Technol.* **1997**, *31* (11), 3180−3187.
(31) Mattia, M.; Tuccimei, P.; Ciotoli, G.; Soligo, M.; Carusi, C.; Rainaldi, E.; Voltaggio, M. Applied Sciences Combining Radon Deficit, NAPL Concentration, and Groundwater Table Dynamics to Assess Soil and Groundwater Contamination by NAPLs and Related Attenuation Processes. 2023, pp 1−18.
(32) Schubert; Freyer, M.; Treutler, H. C.; Weiß, H. Using the Soil Gas Radon as an Indicator for Ground Contamination by Non-Aqueous Phase-Liquids. *J. Soils Sediments* **2001**, *1* (4), 217−222.
(33) Schubert; Peña, M.; Balcázar, M.; Meissner, R.; Lopez, a.; Flores, J. H. Determination of Radon Distribution Patterns in the Upper Soil as a Tool for the Localization of Subsurface NAPL Contamination. *Radiat. Meas.* **2005**, *40* (2−6), 633−637.
(34) Semprini, L.; Istok, J. *Radon-222 as a Natural Tracer for Monitoring the Remediation of NAPL Contamination in the Subsurface*; Corvallis, OR, 2006.

(35) Barbosa, E. Q. Q.; Galhardi, Ja.; Bonotto, D. M. M. The Use of Radon (Rn-222) and Volatile Organic Compounds in Monitoring Soil Gas to Localize NAPL Contamination at a Gas Station in Rio Claro, São Paulo State, Brazil. *Radiat. Meas.* **2014**, *66*, 1−4.
(36) Briganti, A.; Voltaggio, M.; Carusi, C.; Rainaldi, E. Radon Deficit Technique Applied to the Study of the Ageing of a Spilled LNAPL in a Shallow Aquifer ☆. *J. Contam. Hydrol.* **2024**, *263* (April), No. 104342.
(37) Castelluccio, M.; Agrahari, S.; De Simone, G.; Pompilj, F.; Lucchetti, C.; Sengupta, D.; Galli, G.; Friello, P.; Curatolo, P.; Giorgi, R.; Tuccimei, P. Using a Multi-Method Approach Based on Soil Radon Deficit, Resistivity, and Induced Polarization Measurements to Monitor Non-Aqueous Phase Liquid Contamination in Two Study Areas in Italy and India. *Environ. Sci. Pollut. Res.* **2018**, *25* (3), No. 12515.
(38) Cecconi, A.; Verginelli, I.; Baciocchi, R.; Lanari, C.; Villani, F.; Bonfedi, G. Using Groundwater Monitoring Wells for Rapid Application of Soil Gas Radon Deficit Technique to Evaluate Residual LNAPL. *J. Contam. Hydrol.* **2023**, *258* (August), No. 104241.
(39) De Simone, G.; Galli, G.; Lucchetti, C.; Tuccimei, P. Using Natural Radon as a Tracer of Gasoline Contamination. *Procedia Earth Planet. Sci.* **2015**, *13*, 104−107.
(40) De Simone, G.; Lucchetti, C.; Pompilj, F.; Galli, G.; Tuccimei, P.; Curatolo, P.; Giorgi, R. Soil Radon Survey to Assess NAPL Contamination from an Ancient Spill. Do Kerosene Vapors Affect Radon Partition ? *J. Environ. Radioact.* **2017**, *171*, 138−147.
(41) García-González, J.; Ortega, M. F.; Chacón, E.; Mazadiego, L. F.; De Miguel, E.; Miguel, E. De. Field Validation of Radon Monitoring as a Screening Methodology for NAPL-Contaminated Sites. *Appl. Geochem.* **2008**, *23* (9), 2753−2758.
(42) Starr, R. C.Evaluation of the Radon222 Deficit Technique for Delineating DNAPL Distribution and Assessing DNAPL Removal at the OK Tool Source Area, Operable Unit 1, Sacage Municipal Well Superfund Site, Milford, New Hampshire: Final Report. 2007. NWI-2229.180.001.
(43) Barrio-Parra, F.; Izquierdo-Diaz, M.; Díaz-Curiel, J.; De Miguel, E. Field Performance of the Radon Deficit Technique to Detect and Delineate a Complex DNAPL Accumulation in a Multi-Layer Soil Profile. *Environ. Pollut.* **2021**, *269*, No. 116200.
(44) De Miguel, E.; Barrio-Parra, F.; Izquierdo-Díaz, M.; Izquierdo-díaz, M.; Fernández, J.; García-González, J.; García-gonzález, J. E. Applicability and Limitations of the Radon-Deficit Technique for the Preliminary Assessment of Sites Contaminated with Complex Mixtures of Organic Chemicals : A Blind Field-Test. *Environ. Int.* **2020**, *138* (January), No. 105591.
(45) Davis, B. M.; Semprini, L.; Istok, J. Development of Radon as a Natural Tracer for Monitoring the Remediation of NAPL Contamination in the Subsurface. 2002.
(46) Chen, Y.-T.; Tung, T.-H.; Wang, L.-C.; Lu, C.-J. Field Study of Using Naturally Occurring Radon to Assess the Dense Non-Aqueous Phase Liquid Distribution in Saturated Zone. *J. Environ. Radioact.* **2014**, *128*, 75−83.
(47) Kim, J.; Kim, J.; Baek, J.; Shin, J.; Lee, S.; Lee, K. Assessment of Radon Tracer for DNAPL Characterization Within the Groundwater Through Push-Pull Tests. *J. Soil Groundwater Environ.* **2024**, *29* (6), 141−153.
(48) Kim, J.; Kaown, D.; Lee, K. Coupling of Radon and Microbial Analysis for Dense Non-Aqueous-Phase Liquid Tracing and Health Risk Assessment in Groundwater under Seasonal Variations. *J. Hazard. Mater.* **2024**, *475* (February), No. 134939.
(49) Utley, W. S. Creosote. In *Encyclopedia of Toxicology*; Wexler, P., Ed.; Elsevier, 2005; pp 677−678.
(50) Scherr, K. E.; Vasilieva, V.; Lantschbauer, W.; Nahold, M. Composition and Dissolution of a Migratory, Weathered Coal Tar Creosote DNAPL. *Front. Environ. Sci.* **2016**, *4* (SEP), 1−10.
(51) Cheremisinoff, N. P.; Rosenfeld, P.; Davletshin, A. R. The Wood Preserving Industry. *Responsible Care* **2008**, 317−382.
(52) Alden, D. F.; García-Rincón, J.; Rivett, M. O.; Wealthall, G. P.; Thomson, N. R. Complexities of Petroleum Hydrocarbon Contaminated Sites. In *Advances in the Characterisation and Remediation of Sites Contaminated with Petroleum Hydrocarbons (Environmental Contamination Remediation and Management)*; García-Rincón, J.; Gatsios, E.; Lenhard, R.; Atekwana, E.; Naidu, R., Eds.; Springer, 2023.
(53) Miklyaev, P. S.; Petrova, T. B.; Shchitov, D. V.; Sidyakin, P. A.; Murzabekov, M. A.; Tsebro, D. N.; Marennyy, A. M.; Nefedov, N. A.; Gavriliev, S. G. Science of the Total Environment Radon Transport in Permeable Geological Environments. *Sci. Total Environ.* **2022**, *852* (August), No. 158382.
(54) USEPA. EPA's Priority Pollutant List; 2014. https://www.epa.gov/.
(55) Yang, J.; Busen, H.; Scherb, H.; Hürkamp, K.; Guo, Q.; Tschiersch, J. Modeling of Radon Exhalation from Soil Influenced by Environmental Parameters. *Sci. Total Environ.* **2019**, *656*, 1304−1311.
(56) Netto, A. D. P.; Moreira, J. C.; Dias, A. E. X. O.; Ferreira, L. F. V.; Oliveira, A. S. Evaluation of Human Contamination with Polycyclic Aromatic Hydrocarbons (PAHs) and Their Nitrated Derivatives (NHPAs): A Review of Methodology. *Quim. Nova* **2000**, *23* (6), 765−773.
(57) van Noort, P. C. Estimation of Amorphous Organic Carbon/Water Partition Coefficients, Subcooled Aqueous Solubilities, and n -Octanol/Water Distribution Coefficients of Alkylbenzenes and Polycyclic Aromatic Hydrocarbons. *Chemosphere* **2009**, *74* (8), 1018−1023.
(58) RAIS. Risk Assessment Information System. https://rais.ornl.gov/ (accessed Dec 1, 2024).
(59) Newell, C. J.; Acree, D. A.; Randall, R. R.; Huling, S. G. Light Nonaqueous Phase Liquids. *EPA Ground Water Issue* **1995**, 1−28.
(60) Schubert; Freyer; Treutler; WeissRadon-222 as an Indicator of Subsurface NAPL Contamination *Groundwater 2000* 2000, p 2.
(61) Mitev, K.; Dutsov, C.; Georgiev, S.; Boshkova, T.; Pressyanov, D. Unperturbed, High Spatial Resolution Measurement of Radon-222 in Soil-Gas Depth Profile. *J. Environ. Radioact.* **2019**, *196* (January 2018), 253−258.
(62) Mazadiego, L. F. *Desarrollo de Una Metodología Para La Prospección Geoquímica En Superficie de Combustibles Fósiles,*; Universidad Politécnica de Madrid, 1994.
(63) Morse, J. G.; Rana, M. H.; Morse, L. Radon Mapping Aas Indicators of Subsurface Oil and Gas. *Oil Gas J.* **1982**, *80*, 227−246.
(64) Lorenzo, D.; Barrio-Parra, F.; Cecconi, A.; Serrano-García, H.; Izquierdo-Díaz, M.; Santos, A.; De Miguel, E. Enhancing Radon-Deficit Technique Efficacy: Machine Learning Applications for Environmental Variable Analysis in Soil Gas Monitoring. *Environ. Sci. Pollut. Res.* **2025**, *32*, No. 0123456789.
(65) Djeufack, L. B.; Bineng, G. S.; Modibo, O. B.; Ndjana Nkoulou, J. E.; Saïdou. Correlation between Ground 222 Rn and 226 Ra and Long-Term Risk Assessment at the at the Bauxite Bearing Area of Fongo-Tongo, Western Cameroon. *Radiation* **2022**, *2* (4), 387−404.
(66) Lara, E.; Rocha, Z.; Santos, T. O.; Rios, F. J.; Oliveira, A. H. Soil Features and Indoor Radon Concentration Prediction: Radon in Soil Gas, Pedology, Permeability and 226Ra Content. *Radiat. Prot. Dosimetry* **2015**, *167* (1−3), 126−129.

https://doi.org/10.1021/acs.est.5c13917
Environ. Sci. Technol. 2025, 59, 26796−26805